

A Vision-Language Agent System for Compositional Reasoning with VLM-assisted Script and Executable Generation

Yichang Xu¹, Gaowen Liu², Ramana Rao Kompella², Sihao Hu¹,
 Tiansheng Huang¹, Fatih Ilhan¹, Selim Furkan Tekin¹, Zachary Yahn¹, Ling Liu¹

¹Georgia Institute of Technology, Atlanta, GA

²Cisco Systems, USA

{xuyichang, sihaohu, thuang, filhan, stekin6, zachary.yahn}@gatech.edu
 {gaoliu, rkompell}@cisco.com, ling.liu@cc.gatech.edu

ABSTRACT

The advancement in large language models (LLMs) and large vision models has fueled the rapid progress in multi-modal vision-text reasoning capabilities. However, existing vision-language models (VLMs) to date offer poor performance for compositional reasoning. This paper presents VLAgent, a vision-language agent system for vision-text compositional reasoning with three novel features. *First*, VLAgent leverages a pre-trained LLM with few-shot context learning to generate the planning script for each compositional reasoning task and provides a backend engine to generate and perform executable runtime, which maps the planning script into executable code using the VLAgent library for VLAgent executor. *Second*, VLAgent introduces the SS-parser, which identifies and corrects logic errors embedded in the LLM-generated planning script, to further enhance the quality of script-executable mapping. *Third*, VLAgent introduces the compositional reasoning output verifier, which validates and refines the output of complex compositional reasoning steps, by leveraging complementary reasoning techniques, e.g., ensemble learning and caption analysis. Extensive experiments are conducted on six visual benchmarks and compared to a dozen of the SoTA visual reasoning models. The results show that VLAgent outperforms existing representative approaches for compositional text-visual reasoning. Our code and datasets with outputs will be made available upon acceptance.

PVLDB Reference Format:

Yichang Xu¹, Gaowen Liu², Ramana Rao Kompella², Sihao Hu¹,
 Tiansheng Huang¹, Fatih Ilhan¹, Selim Furkan Tekin¹, Zachary Yahn¹, Ling Liu¹. A Vision-Language Agent System for Compositional Reasoning with VLM-assisted Script and Executable Generation. PVLDB, 14(1): XXX-XXX, 2020.

doi:XX.XX/XXX.XX

1 INTRODUCTION

Complex visual reasoning tasks often involve multiple individual models independently trained for different task-specific visual or text processing and reasoning. Hence, learning to perform all tasks in one visual reasoning job end-to-end poses significant challenges to advanced large vision-language models (VLMs), including GPT-5.

This work is licensed under the Creative Commons BY-NC-ND 4.0 International License. Visit <https://creativecommons.org/licenses/by-nc-nd/4.0/> to view a copy of this license. For any use beyond those covered by this license, obtain permission by emailing info@vldb.org. Copyright is held by the owner/author(s). Publication rights licensed to the VLDB Endowment.

Proceedings of the VLDB Endowment, Vol. 14, No. 1 ISSN 2150-8097.
 doi:XX.XX/XXX.XX

To address the technical challenges of compositional visual reasoning, we argue that the next generation of visual reasoning agent systems should provide the following three fundamental compositional reasoning capabilities:

- (1) Robust integration of LLM-based planning script generation for vision-text reasoning task with a concert of back-engine programmable modules and runtime system.
- (2) Systematic deployment of neural-symbolic computation integration on demand, enhanced with comprehensive syntax-semantic parser and error repairer to ensure the correctness of planner-executor mapping and runtime execution.
- (3) Incorporation of agile output auditing and evaluation modules to validate and refine compositional reasoning steps prior to generating the final answer, aiming to fortify the generalization performance of complex visual reasoning.

To date, two threads of research activities have been engaged towards end-to-end visual reasoning. Neural Module Networks (NMN) [2, 3, 14, 15, 19] is pioneering work in the model training category, which aims to address the challenges of end-to-end visual reasoning models by decomposing complex reasoning tasks into modular compositional subroutines through supervised learning with large labeled training datasets. NMN development shows that neural modular networks can significantly improve the interpretability of visual reasoning. Inspired by the ideas of neural modular networks, recent approaches are centered on zero-shot learning, instead of training with supervised learning. Pre-trained LLMs (open source or close source) are utilized to generate structured program steps for performing end to end compositional reasoning. For example, ProgPrompt [37] generates executable programs to help robots perform vision-related tasks. ViperGPT [40] and VisProg [13] aim to solve visual question and answer (VQA) problems with zero-shot learning. ViperGPT formulates Python programs based on existing Python libraries and VisProg uses LLM to generate more structured program that calls external modules and execute the LLM generated program through its Python engine (see Related Work in Section 4 for more detail).

However, existing visual inference methods to date suffer from a number of limitations. *First*, LLM generated programs, though following the structure of in-context learning, often produce non-existent modules or logically flawed execution program steps. *Second*, existing approaches fail to provide the parser and evaluator for checking the validity of LLM generated program w.r.t. both the feasibility of generating runnable execution code and the correctness of visual reasoning output. As a result, existing methods tend to fail miserably when the LLM generated program is ill-formatted or

| | | | | | |
|----------------------|--|---|---|--|--|
| Video | | | | | |
| Video ID | 5188348585 | 6781937922 | 3701219945 | 8568772570 | 3426605205 |
| Question | Did the woman from the driving seat get back in the car after dancing? | How are the identities of the people shown? | What did he do at the end of the video? | What did the lady with green headband do before she released the catapult? | Why does the person wearing bracelet swipe the food away from the baby in the middle of the video? |
| GPT-5 | ✗ | ✗ | ○ | ✗ | ✗ |
| GPT-5-Thinking | ○ | ✗ | ○ | ✗ | ✗ |
| LLaVA-Video-7B-Qwen2 | ○ | ✗ | ✗ | ✗ | ✗ |
| LLaVA-NeXT-Video-7B | ○ | ○ | ○ | ✗ | ✗ |
| LLaVA-NeXT-Video-34B | ○ | ○ | ✗ | ✗ | ✗ |
| InternVL-3.5-8B | ○ | ✗ | ✗ | ✗ | ✗ |
| InternVL-3.5-38B | ○ | ✗ | ✗ | ✗ | ✗ |
| VideoLLAMA3-7B | ○ | ✗ | ○ | ✗ | ✗ |
| VLAgent | ○ | ○ | ○ | ○ | ✗ |

Figure 1: Illustration by examples the performance of eight VLMs on NeXT-QA compared with VLAgent. The raw video is named as “{video_id}.mp4” and can be accessed through the NeXT-QA Google Drive.

logically incorrect. *Finally*, existing approaches tend to hard-wire a pre-defined external module (e.g., pre-trained model) for each specific reasoning step, making their performance bounded to the performance of the weakest external module(s).

Motivated by the above observations, we present VLAgent, a vision-language agent system, for efficient and end-to-end compositional visual reasoning with three novel design characteristics. *First*, the VLAgent leverages a pretrained LLM to create a step-by-step planning script for a visual reasoning request, and develops a VLAgent backend engine to support the mapping of planning steps to executable code and perform runtime execution to generate final output. *Second*, the VLAgent introduces our SS-Parser to improve the quality and correctness of LLM-generated planning scripts prior to generating executable for runtime execution. This SS-Parser inspects and corrects syntactic and semantic errors inherent in the planning steps in the LLM generated program script. *Third but not the least*, the VLAgent provides an output verifier to validate and refine compositional visual reasoning steps to further improve the generalization performance of the final output for each visual reasoning task. Figure 1 illustrates by examples the effectiveness of VLAgent compared with eight VLMs, including GPT-5 and GPT-5-Thinking on NeXT-QA benchmark. VLAgent correctly solves four out of five cases. Extensive experiments are performed on six representative benchmarks, including four image QA benchmarks: GQA [16], NLVR2 [39], VQAv2 [11], and MME [9], one video QA benchmark: NeXT-QA [46], and one complex referring expression benchmark HC-RefLOCO [44]. In image QA datasets, the results demonstrate that the VLAgent consistently outperforms existing zero-shot learning methods by 3% to 40% in terms of accuracy. For video QA, the VLAgent surpasses zero-shot methods by 5% to 17%. For HC-RefLOCO benchmark, VLAgent surpasses the 13 representative SoTA methods by a large margin of 7%.

2 METHODOLOGY

Figure 2 gives an architectural overview of VLAgent. On the left, we show that the VLAgent task planner leverages a pre-trained LLM with few-shot examples for in-context learning (ICL). Both the text-visual reasoning task and the text input of few-shots ICL are fed into the planning script generator, which instructs the LLM to follow the format of few-shot examples to decompose a user-submitted visual reasoning task into a sequence of modular steps in the planning script (top middle box), each corresponds to an external or an internal module (function call) for VLAgent to carry out the respective compositional reasoning task. The SS-Parser (blue) consists of three main VLAgent modules: It first invokes the Script Parser and Script Auditor to examine the generated planning script and detect syntax errors and incorrect program logic. The Script Repair module is triggered to fix errors and generate the correct planning script. Once the SS-Parser completes the syntax-semantic checking and repairing, it will forward the correctness approved script to the VLAgent executor and refinement subsystem (green in the lower right of the figure), which consists of three core modules. It first invokes the Script Executor, which maps the planning script steps to the executable codes to call external modules or internal library functions. Then it will run each executable step by the *Step Executor*. By running the corresponding executable code corresponding to the sequence of steps contained in the planer script, the executor will summarize and generate the final answer. To ensure the robustness and generalization performance of compositional reasoning of VLAgent, we validate the output from the executor through the VLAgent output verifier, which consists of diverse and yet complementary visual reasoning techniques to perform inconsistency resolution with a ranked list of feasible final answers sorted in the descending order of their statistical confidence scores. The result with the highest score is returned as the final answer

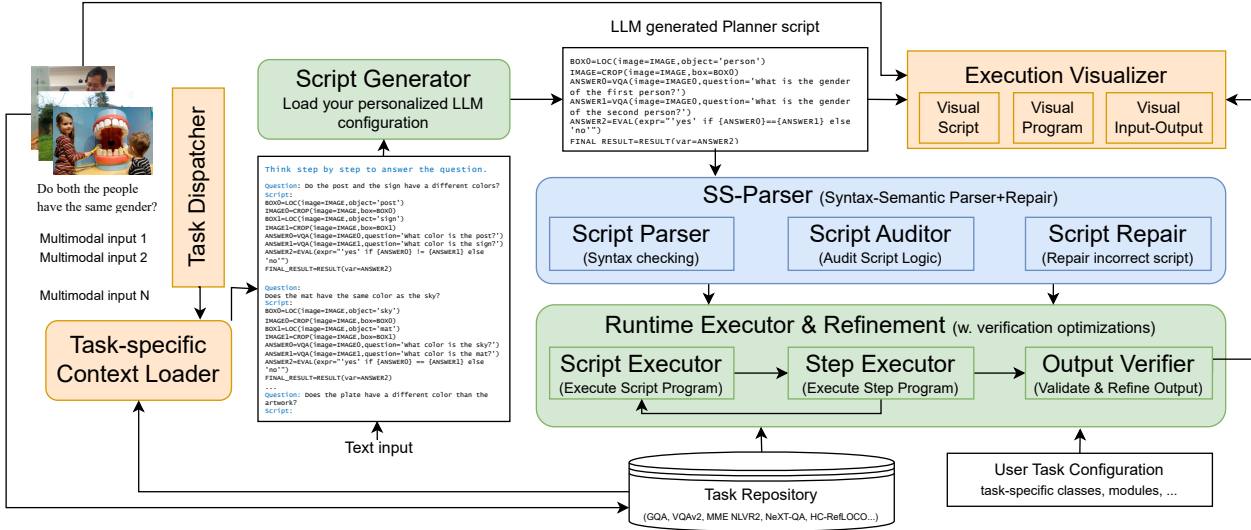


Figure 2: The Architectural Overview of the VLAgent system.

VLAgent recommends to the user. The *Execution Visualizer* (top right) is leveraged for debugging and human-in-the-loop analysis and feedback. All internal and external modules are configurable in VLAgent through the configuration manager. Figure 3 gives a summary of the default module names supported in the alpha version of VLAgent used in the experiments reported in this paper.

2.1 Task Planner

Users can configure the VLAgent task planner by replacing the default LLM in the configuration with his/her favorite LLM for generating planning script for each of his/her visual task. Both in-context learning and prompt engineering techniques are leveraged in VLAgent task planner to improve the quality and reduce syntax or logic errors in the LLM generated scripting program due to weak learning by following instructions by few-shots and unwanted LLM hallucination. Concretely, we combine some effective prompt engineering techniques, such as chain of thought (CoT) and few-shot in-context learning (ICT), to provide higher quality of instructions with fewer examples. By magnifying Figure 2, one can see the in-context learning input to an LLM, which is shown in the text box below the Script Generator. Given a visual reasoning question by user, e.g., “*Do both the people have the same gender*”, the planner feeds the in-context learning instruction to the default or user-chosen LLM, which consists of CoT instruction (“*think step by step to answer the question*”) followed by the K few-shot examples, each in the pair of (question, planning script) where K is one of the configurable hyper-parameters in VLAgent. This input text box guides the chosen LLM to follow the step-by-step instructions shown in the in-context learning examples where different VQA contexts are utilizing different VLAgent internal and external modules. As a result, LLM learns to generate the new planning script with a sequence of compositional program steps for each new zero-shot user’s query. Each line in the planning script corresponds to one instruction (see the example LLM generated script in the top middle text box of Figure 2). Each instruction is expressed as an assignment statement with output variable, the visual processing

module, consisting of module name and its input parameters. All module names used in the K -shot examples are two types: (i) either default or user-chosen external pre-trained models in VLAgent configuration; and (ii) internal modules from the VLAgent Python library.

All K -shot (question, planning-script) examples are stored in the *Task Repository* (recall Figure 2). For each user query, the *Task Dispatcher* will fetch the corresponding set of examples, and the *Task-specific Context Loader* will construct prompt with CoT and K -shot examples followed by user-query and feed them to the given LLM, which learns to generate the task-specific planning script via in-context learning.

2.2 VLAgent Backend Engine

Recall Figure 2, upon the completion of task planner for each text-visual query, the planner will send the generated script to the VLAgent backend execution engine. In order to generate correct executable code for completing the given compositional visual reasoning task, the VLAgent backend engine will first invoke the *SS-Parser* for parsing and detecting both syntax and semantics errors and repair them before passing the planning script to the plan executor. The *SS-Parser* first invokes *Script-Parser* to check the syntax errors of the LLM generated script instruction by instruction. Then it triggers the *Script Evaluator* to identify any logic errors and validate the semantic correctness of the sequence of instructions. Upon detecting errors, the *Script Repair* module will be called to fix both syntax and semantic errors before sending the planning script to the *Script Executor*, which run the corresponding executable code for the sequence of instruction steps by iteratively executing the *Step Executor* and obtaining the processing and reasoning result following the sequence of instruction steps. We further optimize the final answer generated by the VLAgent by employing diverse output verification guards to evaluate the step-wise output consistency through caption-verification and ensemble verification. In the rest of this section, we first motivate the design of our syntax-semantic

| Module Name | Pre-trained models/ Python Modules | Input | Output | Description |
|--------------|---|--|--|--|
| LOC | owlvit-large-patch14 owlv2-large-patch14 owlv2-large-patch14-ensemble grounding-dino-base | Image/video, object name/event | A list of bounding boxes sorted in descending order of scores, or start and end frame of described event | Object detection given an object class, or event location given a description. |
| VQA | blip-vqa-capfilt-large vilt-b32-finetuned-vqa paligemma-3b-ft-vqav2-448 Phi-3.5 (only for video input) | Image/video, question | Answer/Answers in list format for each video frame | Answer visual attributes like color of objects in an image or do per-frame QA given a video. |
| VIDQA | llava-video-7b-qwen2 | Video, question | Answer | Answer questions given a video. |
| CAP | Florence-2 | Image/video | Caption/Per-frame captions | Image captioning. When the input is a video, do per- frame captioning. |
| FIND | clip-vit-large-patch14 | Image, bounding box list, name | Bounding box | Select a bounding box whose content matches the name best. This allows to select a celebrity. |
| SELECT | gpt-4.1-mini | Question, answers from QA modules, choices | Choice index | Given a question and information collected from QA modules, select the best choice. Scores for each choice is also generated and recorded. |
| CROP | PIL.crop() | Image, bounding box list | Image | Crop at the first bounding box in the list. If the list is empty, return the original image. |
| CROP_LEFTOF | PIL.crop() | Image, bounding box list | Image | Get the image to the left of the first bounding box. If the list is empty, return the left part of the image. |
| CROP_RIGHTOF | PIL.crop() | Image, bounding box list | Image | Get the image to the right of the first bounding box. If the list is empty, return the right part of the image. |
| CROP_ABOVE | PIL.crop() | Image, bounding box list | Image | Get the image region above first bounding box. If the list is empty, return the top part of the image. |
| CROP_BELOW | PIL.crop() | Image, bounding box list | Image | Get the image region below first bounding box. If the list is empty, return the bottom part of the image. |
| EVAL | eval() | Expression | Result | Evaluate an expression written in Python syntax. |
| COUNT | len() | Bounding box list | Integer | Count the number of bounding boxes in the list. |
| GET | PIL.Image.size | Image | Bounding box list with one element | Get the bounding box (border) of an image. |
| VOTE | list() | Bounding box lists | Voted bounding box | Given lists of bounding boxes, select a bounding box with highest intersection. |
| CLIP | Video.clip() | Video, start and end of time an event | Clipped video | Clip a video. Here Video is a class in VLAgent to store a video. |
| LENGTH | cv2.VideoCapture.get() | Video | Duration of the video | Get the duration of the video in secs. |
| CLIP_BEFORE | Video.clip() | Video, start and end time of an event | Clipped video | Clip the video before the starting frame. |
| CLIP_AFTER | Video.clip() | Video, start and end time of an event | Clipped video | Clip the video after the starting frame. |
| CLIP_AROUND | Video.clip() | Video, time to clip around | Clipped video | Clip the video around the designated time. |
| RESULT | dict() | Variable name | Value of the variable | Return the value of a runtime variable as the result. |

Figure 3: Core Modules supported in VLAgent. The module names are the naming convention learned by the Planner via a combo of K -shots and CoT for in-context instruction-learning. The first six rows are external pre-trained models marked in blue. The remaining modules marked in green, each corresponds to an internal module in the VLAgent Python library. LOC, VQA, CAP, CROP to GET, and RESULT are used for GQA, VQAv2, MME workloads. For NLVR2 task, only VQA, EVAL and RESULT are used. Video QA task uses modules accepting video as input plus SELECT and EVAL. HC-Ref-LOCO videoQA task uses LOC, CAP, FIND, and VOTE.

parser (SS-Parser) and our output verifier by examples. Then we will give a brief overview of the implementation detail for different components of our script evaluator.

2.2.1 SS Parser. Before passing the planning script to the *Script Executor*, the VLAgent needs to perform syntax and semantic verification for detecting potential syntax errors and logic errors. The *Script Parser* examines the script line by line for syntax errors. For example, it flags any script that uses a non-existent module name or non-existent input parameters. The *Script Auditor* performs semantic-level examination to spot logic operational errors. For

instance, the Script Evaluator will check the object class name parameter in the LOC module, detect incorrect parameters, and repair the errors by generating a correct sequence of instructions.

Figure 4 provides illustration by example on how the task planner works and the effect of SS-Parser on the overall performance of VLAgent. Consider a user query “*Do both the people have the same gender*” with the visual image on the top left. The ground truth answer for this zero-shot VQA is also given under the image in green color. The planning script generated by LLM (GPT-3.5 in this case) is given on the top of Figure 4. This script consists of six lines, calling LOC, CROP, VQA, EVAL and RESULT modules. The overall correct logic is to locate all the people in the image, crop them, ask

Question:
Do both the people have the same gender?



Correct answer: no

```
BOX0=LOC(image=IMAGE,object='person')
IMAGE0=CROP(image=IMAGE,box=BOX0)
ANSWER0=VQA(image=IMAGE0,question='What is the gender of the first person?')
ANSWER1=VQA(image=IMAGE0,question='What is the gender of the second person?')
ANSWER2=EVAL(expr="yes" if {ANSWER0} == {ANSWER1} else 'no')
FINAL_RESULT=RESULT(var=ANSWER2)
```

ANSWER0="female"
ANSWER1="female"
ANSWER2="yes"
FINAL_RESULT="yes" X

```
BOX_ARRAY0=LOC(image=IMAGE,object='person',plural=True)
IMAGE_ARRAY0=CROP(image=IMAGE,box=BOX_ARRAY0)
ANSWER0=VQA(image=IMAGE_ARRAY0,index=1,question='What is the gender of the person?')
ANSWER1=VQA(image=IMAGE_ARRAY0,index=2,question='What is the gender of the person?')
ANSWER2=EVAL(expr="yes" if {ANSWER0} == {ANSWER1} else 'no')
FINAL_RESULT=RESULT(var=ANSWER2)
```

BOX_ARRAY0= 

IMAGE_ARRAY0=[]

ANSWER0="female"
ANSWER1="male"
ANSWER2="no"
FINAL_RESULT="no" ✓

Figure 4: VLAgent performs this visual reasoning task by leveraging its SS-Parser to correct the reasoning error inherent in the LLM-generated planning script.

the gender of each person and compare. However, there is a logical error in the LLM-generated planner script in the 4th step, which leads to a wrong answer.

Concretely, we illustrate the utility of our SS-Parser in evaluating the correctness of LLM-generated planning script and repairing and correcting the planning script by the example in Figure 4. By examining the script at the top, although the intention of the script looks correct, there is a critical logical error: IMAGE0 is cropped by the bounding box with the highest confidence score, which is the girl in the cropped image. Hence, the girl’s gender is asked twice. A main source of the error is the inadequate use of the sequence of instructions when there are more than one objects of the same class to be detected (e.g., people in this query). In order to make the answer correct, we should consider both the bounding boxes with the top two highest scores, and crop both of them respectively, then followed by reasoning on the gender of person in each of the two cropped images. The top rectangle shows the VLAgent without using SS-Parser and in contrast, the bottom rectangle shows the use of SS-Parser to identify and repair the planning script. In this example, VLAgent SS-Parser explicitly uses an array as the output variable for LOC instruction and performs CROP for each of the two bounding boxes in the output array of LOC. Followed by using VQA to ask the gender question on each of the two cropped images in IMAGE_ARRAY0. This enables the EVAL module to compare the gender of the two people. The execution visualization gives intuitive interpretations of the sequence of instructions performed to produce the correct final answer.

2.2.2 Runtime Executor & Output Verifier. As shown on the right middle of Figure 2 in green rectangle, this VLAgent subsystem consists of three core components. The *Script Executor* will be

invoked upon the completion of SS-Parser. It takes as the input a parser-approved planning script and examines each instruction one by one, following the sequence of instruction steps by iteratively calling the *Step Executor*, which locate and run the corresponding external module or the internal executable Python module, including the 21 modules listed in Figure 3. The refinement optimization is designed by a combo of caption verifier and ensemble verifier.

Caption Verifier. In image QA or video QA tasks, for each image or video frame to be processed, we obtain the caption of the input image as a reference point for checking output consistency before generating our final answer for each user query. In the first prototype of VLAgent, we develop the caption verifier using Florence-2 [45]. We first generate a detailed caption of the image or the given video frame, which includes the key elements and their states. Next, a pretrained LLM like GPT-3.5 (chat model) is used to assess whether the caption provides sufficient clues to infer the correct answer. If the caption contains the necessary information, the comparison of the caption-inferred answer is made with the script executor’s output. If the comparison results in a match, indicating the consistency between the execution output and the caption-inferred answer, the final answer is regarded as highly reliable. Otherwise, VLAgent will analyze explicit details in the caption and the caption-derived answer is chosen as the final result if explicit and accurate clues are found in the caption analysis. Table 5 in our ablation study part shows caption verification overall brings non-negligible benefit. **Figure 5** shows an example where the caption-based output verifier corrects the result produced by the script executor. Concretely, upon generating the caption, a consistency checking is performed by a conversation between VLAgent and GPT-3.5. In this dialogue, VLAgent poses three questions: (i)

| | | | |
|---|--|---|--|
| <p>Question: Does the field look grassy?</p>  <p>Correct answer: yes</p> | <p>BOX0=</p>  | <p>IMAGE0=</p>  | <p>ANSWER0="green" ANSWER1="no" FINAL_RESULT="no"</p> <p style="text-align: center;">✗</p> |
| <p>BOX0=LOC(image=IMAGE,object='field') IMAGE0=CROP(image=IMAGE,box=BOX0) ANSWER0=VQA(image=IMAGE0,question='What does the field look like?') ANSWER1=Eval(expr="yes" if {ANSWER0} == 'grassy' else 'no') FINAL_RESULT=RESULT(var=ANSWER1)</p> <p>VLAGent output based on output verification via CapVerif: FINAL_RESULT="yes" ✓ "The image shows a young girl, probably around 4-5 years old, flying a colorful kite in a grassy field..."</p> | | | |

Figure 5: An Example of leveraging our Output Verifier. With the Script Executor obtains "yes" as the result of its execution, the consistency verification using caption and GPT-3.5, our Plan Executor is able to repair the execution result and produce the correct final answer.

does the caption explicitly mention clues to the answer, (ii) which answer is best—between the caption-derived result and the script’s output, and (iii) what is the final answer, stated succinctly. In the illustrated example, if the script returns "no", the output verifier adjusts the result to "yes", since the caption explicitly mentions "a grassy field", a clear and reliable clue. Conversely, if the script executor returns "yes", the caption-verifier also gives "yes" answer, hence, it is deemed as a high confidence answer.

Ensemble Verifier. VLAGent utilizes the ensemble of multiple independently pre-trained models to further enhance the robustness and generalization performance of external module based visual reasoning capabilities, such as class-specific object detection like LOC or visual attribute extraction like VQA by integrating inconsistency resolution with consensus based fusion.

Consider LOC as an example. Suppose we have N models to consider as candidate external modules. Instead of designing an ensemble of N models, we consider only a small subset of M models by ensemble pruning method [6].

For each of the P LOC instructions, we get the bounding box list of M models, denoted as B_{ij} , where $1 \leq i \leq P$, $1 \leq j \leq M$. Let B denote the final list of the M bounding boxes produced by the ensemble fusion of M external LOC models, which serves as a *pseudo label*. Let $Area(B) := \{(x, y) | \exists b \in B, (x, y) \in b\}$ denote the union region of bounding boxes in bounding box list B . Hence, we can compute the confidence score I_{ij} for each bounding box list B_{ij} ($1 \leq i \leq P$, $1 \leq j \leq M$), as follows:

$$I_{ij} = \frac{|Area(\cup B_{ij}) \cap Area(\cup B)|}{|Area(\cup B_{ij}) \cup Area(\cup B)|} \quad (1)$$

which is the Intersection of Union (IoU) between the M bounding boxes in B_{ij} and pseudo label. $|\cdot|$ is the area. We then use the

average IoU of the j th model as its score:

$$s_j = \frac{1}{n} \sum_{i=1}^n I_{ij} \quad (2)$$

After getting $\{s_j\}_{j=1}^N$, we do clustering and select the cluster with the highest scores.

First, we dynamically compute the best K for K-Means [27] algorithm using Silhouette distance [34]:

For each $K \in \{1, 2, 3, \dots, N\}$:

We do K-Means clustering and get K clusters $\{C_r\}_{r=1}^K$. Denote the cluster index for s_j as $C(s_j) \in \{1, 2, \dots, K\}$.

Intra-cluster distance for s_j :

$$a(j) = \frac{1}{|C(s_j)| - 1} \sum_{s_k \in C(s_j), k \neq j} |s_j - s_k| \quad (3)$$

Inter-cluster distance for s_j :

$$b(j) = \min_{r \neq C(s_j)} \frac{1}{|C_r|} \sum_{s_k \in C_r} |s_j - s_k| \quad (4)$$

If $|C(s_j)| = 1$, then the Silhouette distance of s_j is $s(j) = 0$. Otherwise,

$$s(j) = \frac{b(j) - a(j)}{\max\{a(j), b(j)\}} \quad (5)$$

The average Silhouette distance for this K -clustering is

$$S(K) = \frac{1}{N} \sum_{j=1}^N s(j) \quad (6)$$

The best K is chosen as

$$K^* = \arg \max_{K \in \{1, 2, 3, \dots, N\}} S(K) \quad (7)$$

After that, we can do a K^* -Means clustering, and select the cluster C^* which contains largest s_k s. Suppose we aim to select at least M

models. If $|C^*| \geq M$, then the selection ends. Otherwise, run the same algorithm on the remaining models until we finally select at least a total of M models. For VQA, we run the same algorithm. The only difference is I_{ij} is computed as $\mathbb{I}[|A_{ij} \cap A| > 0]$, where A_{ij} is the set of words generated by model j on i -th data, and A is the set of words in the ensembled answer. The detailed algorithm is presented in Algorithm 1 (with LOC as example). The effectiveness of ensemble verifier is measured in the Ablation study in Section 3.2.

Algorithm 1: Model Selection via IoU-based Scoring and K-Means Clustering

Input: N models; m samples from dataset; minimum number of models M

Output: \mathcal{S} : set of selected model indices

- 1 Initialize $\mathcal{S} \leftarrow \emptyset$, $\mathcal{R} \leftarrow \{1, 2, \dots, N\}$
- 2 **while** $|\mathcal{S}| < M$ and $\mathcal{R} \neq \emptyset$ **do**
- 3 Sample m data points and run LOC for n total lines
- 4 **for** $i = 1$ to n **do**
- 5 **for** $j \in \mathcal{R}$ **do**
- 6 Get bounding box list B_{ij} from model j
- 7 Run ensemble algorithm to get pseudo label B_i
- 8 **for** $j \in \mathcal{R}$ **do**
- 9 **for** $i = 1$ to n **do**
- 10 $I_{ij} = \frac{|Area(\cup B_{ij}) \cap Area(\cup B_i)|}{|Area(\cup B_{ij}) \cup Area(\cup B_i)|}$
- 11 $s_j = \frac{1}{n} \sum_{i=1}^n I_{ij}$
- 12 **for** $K = 1$ to $|\mathcal{R}|$ **do**
- 13 Run K-Means clustering on $\{s_j\}_{j \in \mathcal{R}}$ to get clusters $\{C_r\}_{r=1}^K$
- 14 **for** $j \in \mathcal{R}$ **do**
- 15 **if** $|C(s_j)| = 1$ **then**
- 16 $s(j) = 0$
- 17 **else**
- 18 $a(j) = \frac{1}{|C(s_j)|-1} \sum_{s_k \in C(s_j), k \neq j} |s_j - s_k|$
- 19 $b(j) = \min_{r \neq C(s_j)} \frac{1}{|C_r|} \sum_{s_k \in C_r} |s_j - s_k|$
- 20 $s(j) = \frac{b(j) - a(j)}{\max\{a(j), b(j)\}}$
- 21 $S(K) = \frac{1}{|\mathcal{R}|} \sum_{j \in \mathcal{R}} s(j)$
- 22 $K^* = \arg \max_{K \in \{1, 2, \dots, |\mathcal{R}|\}} S(K)$
- 23 Run K^* -Means clustering on $\{s_j\}_{j \in \mathcal{R}}$
- 24 $C^* = \arg \max_{r \in \{1, \dots, K^*\}} \max_{j: C(s_j) = r} s_j$
- 25 $\mathcal{S} \leftarrow \mathcal{S} \cup \{j : C(s_j) = C^*\}$
- 26 $\mathcal{R} \leftarrow \mathcal{R} \setminus \{j : C(s_j) = C^*\}$
- 27 **return** \mathcal{S}

3 EXPERIMENTS

We report the performance evaluation of VLAgent and the comparison with the state-of-the-art representative visual reasoning methods on six benchmarks: four in the image QA domain and two in video QA domain. They are GQA [16], NLVR2 [39], VQAv2 [11] and MME [9] (existence, position, color category), and video QA benchmark NeXT-QA [46] and benchmark HC-RefLOCO [44]. All

experiments are conducted on PACE (Georgia Tech data center) with H100 or H200 GPU in a Python 3.9 environment.

3.1 Experimental Comparison Results

Table 1: Comparing VLAgent with 8 representative methods (VLMs and Zero-Shot) on four benchmarks. Improvement on ZS is the min or max improvement compared to ZS methods. Improvement min and max are the lower and upper bound on improvement over all VLMs or ZS methods.

| Method | NLVR2 | GQA | VQAv2 | MME |
|-----------------------------|---------------|---------------|---------------|---------------|
| BLIP-VQA-Capfilt [23] (sup) | 44.8% | 54.5% | 81.2% | 82.8% |
| Vilt-b32 [21] (VLM) | 46.6% | 51.4% | 73.6% | 74.8% |
| PaliGemma2 [38] (VLM) | 44.4% | 44.5% | 46.5% | 61.6% |
| InternVL3 [8] (VLM) | 50.6% | 61.9% | 61.4% | 84.1% |
| MiniCPM-V-4.5 [48] (VLM) | 51.2% | 70.8% | 68.9% | 85.7% |
| Phi-3.5 [1] (VLM) | 64.5% | 72.7% | 65.5% | 86.0% |
| ViperGPT [40] (ZS) | — | 35.5% | 37.4% | 58.1% |
| VisProg [13] (ZS) | 69.3% | 54.3% | 72.3% | 85.3% |
| GENOME [7] (ZS) | — | 44.7% | 60.5% | 77.9% |
| VLAgent (ZS) | 74.1% | 61.9% | 76.9% | 88.4% |
| Improvement on ZS (min) | +4.8% | +7.6% | +4.6% | +3.1% |
| Improvement on ZS (max) | +4.8% | +26.4% | +39.5% | +30.3% |
| Improvement (min) | +4.8% | -10.8% | -4.3% | +2.4% |
| Improvement (max) | +29.7% | +26.4% | +39.5% | +30.3% |

Table 2: Performance of VLAgent compared with 11 representative methods in VLMs category (top 6 rows) and zero-shot agent methods (middle 5 rows). Hard Split-T means temporal reasoning questions and Hard Split-C means causal reasoning questions. "Overall" represents for the overall accuracy of all types of questions.

| Method | Hard Split-T | Hard Split-C | Overall |
|---------------------------|---------------|---------------|---------------|
| LLaVA-Video-7B-Qwen2 [53] | 60.4% | 69.5% | 70.9% |
| LLAva-NeXT-Video-7B [52] | 54.8% | 65.3% | 65.8% |
| LLAva-NeXT-Video-34B [52] | 55.0% | 63.8% | 61.8% |
| InternVL-3.5-8B [42] | 58.6% | 66.5% | 68.1% |
| InternVL-3.5-38B [42] | 61.1% | 65.8% | 68.8% |
| VideoLLaMA3-7B [51] | 66.3% | 68.0% | 72.2% |
| ViperGPT [40] (ZS) | 48.7% | 56.2% | 56.9% |
| SeViLA [50] (ZS) | 59.6% | 58.5% | 64.0% |
| VideoAgent [43] (ZS) | 60.0% | 68.3% | 66.1 % |
| TravelLER [35] (ZS) | 56.9% | 65.4% | 66.0% |
| MoReVQA [28] (ZS) | 64.6% | 70.2% | 69.2% |
| VLAgent | 65.3% | 71.5% | 74.1% |
| Improvement on ZS (min) | +0.7% | +1.3% | +4.9% |
| Improvement on ZS (max) | +16.6% | +15.3% | +17.2% |
| Improvement (min) | -1.0% | +1.3% | +1.9% |
| Improvement (max) | +16.6% | +15.3% | +17.2% |

This section reports on the experimental comparison of VLAgent with representative SOTA approaches on 6 benchmarks. **Table 1** compares VLAgent with existing representative image QA approaches in both VLMs category and zero-shot inference methods on four

Table 3: Comparison of VLAgent on HC-RefLOCO with 13 SOTA methods (zero-shot or VLMs).

| Model | Acc0.5 | Acc0.75 | Acc0.9 | mAcc |
|--------------------------|---------------|---------------|---------------|---------------|
| GPT-4V [30] | 17.4% | 2.6% | 0.3% | 5.5% |
| GroundingGPT [24] | 56.6% | 27.2% | 5.3% | 29.8% |
| Ferret 13B [49] | 52.9% | 38.5% | 15.6% | 35.7% |
| KOSMOS-2 [31] | 45.3% | 38.0% | 20.0% | 34.1% |
| Qwen-VL [5] | 67.9% | 56.8% | 34.8% | 52.8% |
| OFA-Large [41] | 70.5% | 61.6% | 44.0% | 58.1% |
| SPHINX [25] | 77.5% | 61.0% | 27.0% | 55.4% |
| SPHINX-1K [25] | 80.7% | 68.6% | 41.1% | 63.0% |
| SPHINX-v2-1K [25] | 84.1% | 77.1% | 56.2% | 71.7% |
| PixelLM 13B [33] | 63.6% | 46.6% | 25.8% | 44.6% |
| LISA [22] | 52.4% | 42.1% | 31.3% | 41.1% |
| PSALM [54] | 61.7% | 53.6% | 40.2% | 51.1% |
| GlaMM [32] | 66.1% | 56.9% | 44.2% | 55.0% |
| VLAgent | 82.6% | 77.4% | 63.2% | 73.9% |
| Improvement (min) | -1.5% | +0.3% | +7.0% | +2.2% |
| Improvement (max) | +65.2% | +74.8% | +62.9% | +68.4% |

popular ImageQA benchmarks. We observe that existing zero-shot methods, represented by ViperGPT [40] and Visprog [13], exhibit a significant performance gap compared to supervised fine-tuning approaches. In comparison, VLAgent as a zero-shot approach achieves superior performance for NLVR2 and MME and comparable performance for GQA and VQAv2. Concretely, for VQAv2, VLAgent outperforms the SOTA zero-shot methods (ViperGPT, VisProg and GENOME) by 5 ~ 40%. VLAgent reduces the margin to about 4% w.r.t. the supervised model BLIP-VQA-Capfilt [23] (which is directly finetuned on VQAv2), and outperforms the other VLMs by about 10 ~ 30%. For GQA, VLAgent achieves an accuracy of 61.9%, which outperforms three zero-shot methods by 7.6 ~ 26.4%, and outperforms BLIP-VQA-Capfilt (supervised) and two other VLMs Vilt-b32 and PaliGemma2 by 10.5 ~ 17.4%. VLAgent offers on-par performance to InternVL3 and narrows the gap of all zero-shot methods to MiniCPM-V-4.5 (70.8%) and Phi-3.5 (72.7%) by a large margin (61.9% vs 35.5 ~ 54.3%). For the MME benchmark, VLAgent outperforms all methods compared by achieving an accuracy of 88.8%, including all three zero-shot methods (ViperGPT, VisProg, GENOME), the supervised BLIP-VQA-Capfilt, and the four VLMs. The second best performing model under MME is the VLM by Microsoft Phi-3.5 (86%). For NLVR2 benchmark, VLAgent outperforms all methods compared by a large margin of in accuracy (74.1% vs 44.4 ~ 69.3%).

We also evaluate the generalization capability of VLAgent for VideoQA benchmarks. Due to different ways of testing the two VideoQA benchmarks, we report our experiments on NeXT-QA and HC-RefLOCO in Table 2 and Table 3 respectively. For NeXT-QA video understanding benchmark [46], we sample 200 questions per type from the test set, resulting in a test set of 1493 questions. Table 2 shows the comparison result of VLAgent with six VLMs and five VideoQA specific agent-based methods (zero-shot). VLAgent exhibits a high accuracy on all hard splits and achieves an overall accuracy of 74.1%, surpassing all 11 methods compared, the gain margin is 0.7 ~ 16.6%. For HC-RefLOCO [44], representing the complex referring expression benchmark on long descriptions, we sampled 1400 referring expressions from the test set to test VLAgent. Unlike

traditional referring expression datasets like RefLOCO [20] which are already saturated in terms of performance due to the emergence of expression-based grounding models (such as OWLV2 [29] and Grounding Dino [26] used in this paper), HC-RefLOCO grounds a person with fine-grained description of appearance, position, movement, and so on, posing a great challenge to grounding models. For each video-text reasoning task in HC-RefLOCO, we perform the caption-verification as follows: we first use the LLM to identify the person whose caption best matches the description; if no match is found, then we skip the verification. We then check whether the bounding box of this person substantially overlaps with the predicted result. If yes, the prediction is considered correct. Otherwise, we compare the caption of the predicted bounding box with the description and make the reasoning to produce the final alignment, and we correct the bounding box only when it aligns significantly worse than the caption of the originally selected person. Table 3 shows the performance of VLAgent in HC-RefLOCO compared to the 13 representative methods, of which SPHINX-v2-1K [25] is the well-known state-of-the-art method. Following the metrics in [44], Acc0.5, Acc0.75, Acc0.9 and mAcc are used to measure and compare the performance. AccX means the ratio of test cases whose IoU is greater than X, and mAcc is the average value of Acc0.5 through Acc0.95 with a step size of 0.05. It is observed that even though VLAgent is using lightweight object detection models for inference time efficiency, its Acc0.75, Acc0.9 and mAcc still surpass the 13 SOTA approaches compared. Especially, Acc0.9 has a performance gain over the top performer SPHINX-v2 by about 7%.

3.2 Ablation Study

We organize the ablation study measurement in three ways. First, we compare VLAgent without SS-Parser and output verification optimizations to the full fledged VLAgent, which has all four core components: (i) LLM-based planner to generate reasoning script by following instructions in few-shot with Chain of thought, (ii) SS-Parser, (iii) Script (plan) Executor, and (iv) Output verifiers. This ablation mainly tests the effectiveness of SS-Parser and output verification on the overall performance of the VLAgent system. We also select four representative and popular LLMs for this first study: gpt-3.5-turbo-instruct, Mistral-Small-24B-Base-2501 [18], GLM4-9B [10], and Llama3-8B [12].

Table 4 reports the comparison results of full-fledged VLAgent with its naive version with only LLM-generated script and its runtime executor (w/o parsers and verifiers) with four popular LLMs as the LLM-script generator respectively and tested on all four ImageQA benchmarks. VLAgent consistently outperforms its naive version by a significant margin. In particular, for NLVR2 with GLM, the combo performs poorly with only an accuracy of 19.2% due to incorrect generation of LLM programs. In comparison, VLAgent achieves an accuracy of 58.6% with 39.3% gain margin. Similarly, for VQAv2, VLAgent significantly improves the accuracy with Llama by 14%, Mistral by 6.4%, GPT-3.5 by 4.6%, and GLM by 3.9%. For MME, the full-fledged VLAgent remains the top performer with 3.5% improvement on average. Given that the questions in the selected categories of MME are significantly simpler compared to those in GQA, the naive VLAgent can achieve very good accuracy. The improvement brought by the combo of SS-Parser and Output verifier is about 1 ~ 7%.

Table 4: Accuracy Comparison on 4 benchmarks (GQA, VQAv2, MME, NLVR2). Each benchmark is tested using four different LLMs as the corresponding initial task plan generators for both VLAgent naive (with only LLM script planner and executor) and VLAgent (the full fledged version with SS-Parser and caption and ensemble Verifiers). A total of 16 combos for VLAgent to compare with 16 combos of VLAgent naive, showing the consistent gain of SS-Parser and Output Verifiers.

| Agent Framework | Benchmark | GPT 3.5 | Llama | Mistral | GLM |
|---------------------|-----------|--------------|---------------|--------------|---------------|
| VLAgent naive | GQA | 54.4% | 54.1% | 55.2% | 54.7% |
| | GQA | 61.9% | 58.7% | 60.7% | 60.4% |
| | GQA | +7.5% | +4.6% | +5.5% | +5.7% |
| VLAgent | VQAv2 | 72.3% | 61.0% | 70.8% | 74.2% |
| | VQAv2 | 76.9% | 75.3% | 77.2% | 78.1% |
| | VQAv2 | +4.6% | +14.3% | +6.4% | +3.9% |
| VLAgent Improvement | MME | 86.9% | 81.0% | 85.3% | 86.0% |
| | MME | 88.4% | 88.6% | 88.8% | 87.4% |
| | MME | +1.5% | +7.6% | +3.5% | +1.4% |
| VLAgent | NLVR2 | 69.3% | 65.9% | 67.6% | 19.2% |
| | NLVR2 | 73.2% | 70.0% | 74.1% | 58.6% |
| | NLVR2 | +3.9% | +4.1% | +6.5% | +39.4% |

The next experiment in our ablation study is to further validate the effectiveness of caption-verifier and ensemble-verifier. **Table 5** reports the results. The performance of VLAgent improves progressively with the addition of SS-Parser and caption-verifier (row 2) and the addition of ensemble-verifier (row 3), compared to the naive version of VLAgent without SS-parser and output verifiers.

Table 5: Ablation study (GQA)

| Method | GPT 3.5 | Llama | Mistral | GLM |
|------------------------------|------------------------------|------------------------------|------------------------------|------------------------------|
| VLAgent naive | 54.4% | 54.1% | 55.2% | 54.7% |
| VLAgent +parser+cap-verf | 58.9% +4.5% | 56.9% +2.8% | 58.6% +3.4% | 58.2% +3.5% |
| VLAgent +parser+cap+ensemble | 61.9% +7.5% | 58.7% +4.6% | 60.7% +5.5% | 60.4% +5.7% |

Figure 6 illustrates the effect of ensemble-verifier by an example from GQA with visualization. It shows that with ensemble verification, VLAgent can further improve the LOC performance using three external object detection models chosen by our ensemble-verifier. The cutting board bounding box in BOX1 gets the highest ensemble confidence score based on inconsistency resolution and fusion analysis. As we can see from the figure, the script locates the serving tray and cutting board, and then queries and compares their colors, which is correct. However, the default LOC module in VLAgent returns a wrong bounding box when it performs inference to locate the cutting board, making IMAGE1 remains to be a serving tray, and thus outputs a wrong result. By leveraging two other LOC modules, VLAgent can verify the output of the original LOC module. As shown in the bottom of Figure 6, both of the additional LOC modules can successfully locate the cutting board. As a result, the cutting board is the top-1 bounding box ranked by the fusion confidence score instead of the serving tray, delivering the correct final result by VLAgent with ensemble boosting.

The third experiments we want to report as a part of the ablation study is the latency of each core component and each optimization,

Table 6: Inference time per sample. VLAgent w. parallel means part of the caption verifier runs in parallel with the other VLAgent components.

| Component | Time Cost (s) |
|-------------------------------|---------------|
| VLAgent Naive | 3.24 |
| VLAgent (all) sequential | 7.54 |
| VLAgent (all) Parallel | 5.10 |
| Task Planning | 1.50 |
| LOC (single) | 0.23 |
| LOC (ensemble) | 0.88 |
| VQA (single) | 0.17 |
| VQA (ensemble) | 0.23 |
| SS-Parser | 0.00 (0.0016) |
| Caption Verifier | 4.01 |

especially the cost of ensemble verifier and caption verifier. **Table 6** reports the per-sample inference time of VLAgent on GQA, including its naive version (planner+executor only), and the individual core components within VLAgent. It is observed that empowered with all the SS-parser checking, repairing, and verifying mechanisms, VLAgent runs at 7.54 seconds per sample. Compared to the VLAgent naive which takes 3.24 seconds, the full-fledged VLAgent offers the inference latency at an acceptable range in practice. Also the breakdown of the components reveals that a majority of the added latency stems from the caption verifier, which invokes both an image captioning model and an LLM. In comparison, the ensemble fusion of vision models introduces only a modest overhead and the SS-Parser incurs negligible additional cost.

Important to note is that the captioning and its analysis are independent of script generation and script execution, we can process them in parallel. For parallel implementation of caption-verifier, the total inference time of VLAgent can be reduced to 5.10 seconds

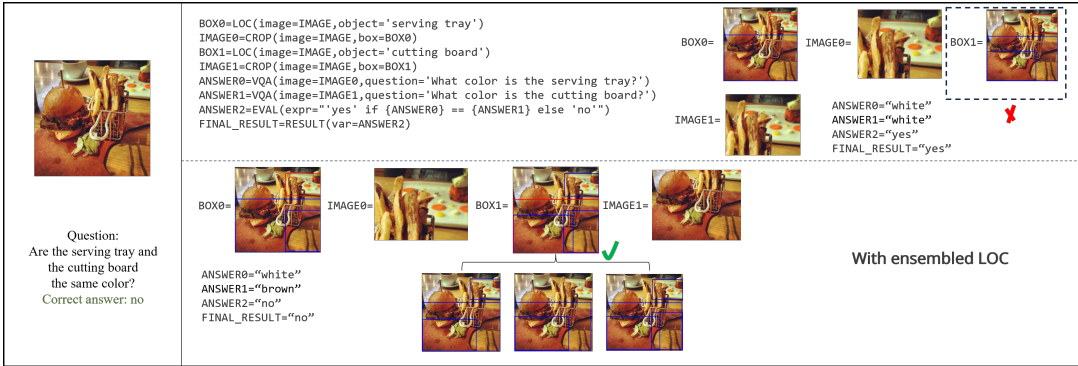


Figure 6: A GQA example illustrates the effectiveness of ensemble verification in VLAgent.

| Image | | | | | | |
|----------------|--|--|---|-------------------------------------|---|---|
| Question | Do both the people have the same gender? | Does the stove top have the same color as the stove? | What is the name on the front of the train? | Are the girls sitting on a railing? | Is there a brown scarf in the image? Please answer yes or no. | Is the monitor on top of a person? Please answer yes or no. |
| Answer | no | no | trimet | no | no | yes |
| BLIP | ✗ (yes) | ✗ (yes) | ✗ (first) | ✗ (yes) | ✗ (yes) | ✗ (no) |
| VisProg | ✗ (yes) | ✗ (yes) | ✗ (first) | ✗ (yes) | ✗ (yes) | ✗ (no) |
| InternVL-3 | ○ (no) | ✗ (yes) | ○ (TriMet Max) | ✗ (yes) | ✗ (yes) | ✗ (no) |
| Phi-3.5 | ○ (no) | ✗ (yes) | ✗ (TRIOMET MAX) | ✗ (yes) | ○ (no) | ○ (yes) |
| GPT-4o | ✗ (unknown) | ✗ (yes) | ○ (TriMet Max) | ○ (no) | ○ (no) | ✗ (no) |
| GPT-5 | ✗ (unknown) | ✗ (yes) | ✗ (EXPO CENTER) | ○ (no) | ○ (no) | ✗ (no) |
| GPT-5-Thinking | ○ (no) | ○ (no) | ✗ (MAX) | ○ (no) | ○ (no) | ✗ (no) |
| VLAgent | ○ (no) | ○ (no) | ○ (TriMet Max) | ○ (no) | ○ (no) | ○ (yes) |

Figure 7: Six cases showing the correctness of BLIP [23], VisProg [13], InternVL-3 [8], Phi-3.5 [1], GPT-4o, GPT-5, GPT-5-Thinking and VLAgent on single image QA tasks. From left to right are GQA, VQAv2 and MME, showing 2 cases for each.

per sample (a gain margin of 2.44 seconds). This also indicates that the checking and verifying mechanism only adds a tiny latency increase (less than 2s), while offering substantially improved visual compositional reasoning capability and improved interpretability.

3.3 Performance Comparison by Visualization

In this section, we provide some visual illustrations of the performance comparison results in the previous sections. Figure 7 illustrates the comparison results of Table 1 with two examples per benchmark from GQA (columns 2 3), VQAv2 (columns 4 5) and MME (columns 6 7). Each example gives a non-trivial text-visual reasoning query. In all six cases, standard VQA models (incl. ensemble VQA method) fail to produce the correct answers, exposing their limitations in performing compositional visual reasoning tasks. Even models trained with a massive amount of data tend to fail on certain cases. GPT-4o failed on three out of these six queries. GPT-5 failed on four out of the six queries. Even GPT-5-Thinking only achieves good performance in four out of six cases. Consider the query in the column 7, the visual image shows clearly where

the monitor is but GPT-5-Thinking failed on this visual reasoning. In contrast, VLAgent utilizes lightweight external models, and succeeds on all six cases. This showcases that VLAgent and its neuro-symbolic programmable and composable modularity design can offer robust compositional reasoning for zero-shot inference.

Figure 8 illustrates a representative text-video reasoning task with the query “*what did the man in red do right before he started running?*”. The ground truth provided by NeXT-QA is given below the query with B as the correct answer (highlighted in green) out of the five multiple choice answers. In this example, the movement of the man in red is fast, such that we can only infer it from the overall movement in the entire video. Recall Table 2, all existing 11 VLM or zero-shot methods failed. Even GPT-5-Thinking failed in this case as well: GPT-5-Thinking wrongly chooses C as its final answer. In comparison, VLAgent first locates the event where the man has started running and clips the video segment before that. Then the default VideoQA model (VIDQA) is called to answer the question. Due to the fast movement of the man in red, the VideoQA module is unable to reason the correct action of the man in red, whereas VLAgent can identify and crop a short video segment

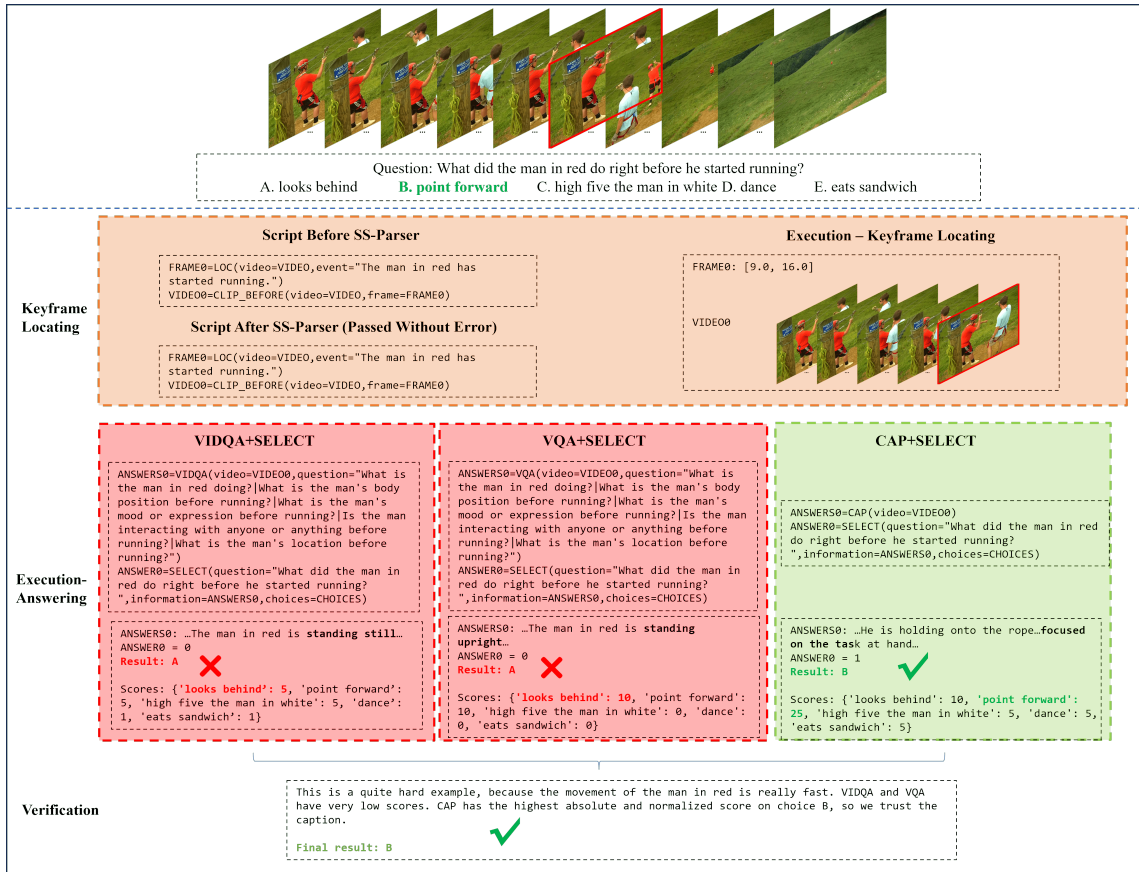


Figure 8: VLAgent example on video QA.

through few-shot and CoT in context learning and then leverage the caption-verifier via the image captioning module to acquire some useful information that implicitly supports the choice B, through our verification-confidence ranking, which shows the likelihood of B larger than other choices. Therefore, VLAgent generates the correct final answer to this question.

Figure 9 provides two examples taken from the case study on NeXTQA in the Introduction (Figure 1) to further illustrate the effectiveness of VLAgent with VideoQA examples. Here, we provide the question, choices, answer, and output for five models/methods for each example. For the first example (top two rows), VLAgent succeeds in asking more questions about the image. Since people are interacting with each other using a tablet and the other four choices are irrelevant in both text query and video (a sequence of video frames), VLAgent is able to conduct compositional visual reasoning to make the correct choice. In contrast, the other 4 models (GPT-5, GPT-5-Thinking, VideoLLAMA3-7B, InternVL-3.5-38B) all failed because they failed to perform compositional visual reasoning to find useful visual clues. In the second example (bottom two rows), VLAgent made the correct choice of E (squat down). However, all other four models (GPT-5, GPT-5-Thinking, VideoLLAMA3-7B, InternVL-3.5-38B) failed with the wrong choice B (pull). One possible analysis is that the four models simply capture the coarse movement of the lady wearing the green headband, i.e., pulling the catapult, but all

failed to capture/identify the squatting body position right before she releases the catapult. These two examples further illustrate with visualization the effectiveness of putting the four core components of VLAgent (LLM-planner, SS-parser, Script Executor, and Output verifiers) in concert.

Recall Figure 1, VLAgent failed to perform correct compositional reasoning on the example in column 6 (the last one on the right). Although all other eight VLM models also failed, it is a representative case where VLAgent could further improve its compositional visual reasoning capability.

4 RELATED WORKS

Our work is inspired by several pioneering projects in Neural Module Networks (NMNs) [3, 14, 15, 19]. NMNs were introduced to improve interpretability by decomposing visual reasoning into explicit sub-tasks. In NMN frameworks, a question is parsed into a layout of modular operations (e.g., find, filter, count), each of which is handled by specialized neural units, and the results are composed to produce the answer. This compositional design yields a step-by-step reasoning trace that is more transparent than monolithic end-to-end models. However, NMNs require supervised learning to train the module selection or layout predictor, often relying on ground-truth programs or strong annotations. Consequently, their generalization is constrained by the quality and quantity of



Figure 9: Two examples comparing VLAgent with four selected approach in detail.

training data, and hard to extend to new tasks without additional supervision. The recent progress in Neural Module Networks includes ViperGPT [40], VisProg [13] and GENOME [7]. These recent projects formulate Python programs that invoke external trained models and Python library modules to obtain answers in visual reasoning tasks.

Our research is also inspired by recent research in LLM enhancement for visual reasoning [13, 37, 40, 47] without task-specific model training or supervised finetuning of foundation models [4, 17, 36]. The visual inference methods prompt an LLM to output an explicit sequence of operations that can invoke pre-built executable modules. ProgPrompt [37] uses an LLM to produce robot task plans as executable code given high-level instructions. PICa [47] introduces the representation of visual information as text via objects and their attributes detected, and it improves the in-context learning with the additional textual data to GPT-3 to obtain answer to a visual question. ViperGPT [40] formulates visual questions as Python programs calling vision APIs to generate answers via code execution. VisProg [13] introduced a well-structured program instruction template for visual reasoning and an interpreter is to execute the external pre-trained vision model or a Python module in Python library. GENOME [7] extends Visprog to unseen task scenarios by adding a process to create new modules and new in-context learning examples. However, most existing zero-shot approaches suffer from the problem of blindly entrusting LLM generated programs, instead of integrating error checking and repairing with result verification as the preconditions for invoking program execution, minimizing the detrimental effect of logical errors in LLM-generated programs,

such as incorrect planning steps, non-existent external modules due to undesirable LLM hallucination.

5 CONCLUSION

We have presented VLAgent, a visual-language agent system for visual-text compositional reasoning. This paper makes three novel contributions. (1) We introduce the novel architectural design of VLAgent, which leverages LLM with few-shot and CoT in-context learning to generate the planning script for each compositional reasoning task and provides a backend engine to generate executable code and run script executor. (2) We develop the SS-parser to empower VLAgent to detect and correct logic errors in the LLM-generated planning script. (3) We develop caption verifier and ensemble verifier to further improve the compositional reasoning performance of VLAgent. Extensive experiments were conducted on six visual benchmarks. We show that VLAgent outperforms existing representative approaches for compositional text-visual reasoning, compared to a dozen of SoTA visual reasoning models.

REFERENCES

[1] Marah Abdin, Jyoti Aneja, Hany Awadalla, Ahmed Awadallah, Ammar Ahmad Awan, Nguyen Bach, Amit Bahree, Arash Bakhtiari, Jianmin Bao, Harkirat Behl, et al. 2024. Phi-3 technical report: A highly capable language model locally on your phone. *arXiv preprint arXiv:2404.14219* (2024).

[2] Jacob Andreas, Marcus Rohrbach, Trevor Darrell, and Dan Klein. 2016. Learning to Compose Neural Networks for Question Answering. In *Proceedings of the 2016 Conference of the North American Chapter of the Association for Computational Linguistics: Human Language Technologies*, Kevin Knight, Ani Nenkova, and Owen Rambow (Eds.). Association for Computational Linguistics, San Diego, California, 1545–1554. <https://doi.org/10.18653/v1/N16-1181>

[3] Jacob Andreas, Marcus Rohrbach, Trevor Darrell, and Dan Klein. 2016. Neural module networks. In *Proceedings of the IEEE conference on computer vision and pattern recognition*. 39–48.

[4] William T Freeman Antonio Torralba, Phillip Isola. 2024. Foundations of computer vision. *MIT Press* (2024).

[5] Jinze Bai, Shuai Bai, Shusheng Yang, Shijie Wang, Sinan Tan, Peng Wang, Junyang Lin, Chang Zhou, and Jingren Zhou. 2023. Qwen-VL: A Versatile Vision-Language Model for Understanding, Localization, Text Reading, and Beyond. *arXiv preprint arXiv:2308.12966* (2023).

[6] Boyu Chen, Zhengrong Yue, Siran Chen, Zikang Wang, Yang Liu, Peng Li, and Yali Wang. 2025. Lvagent: Long video understanding by multi-round dynamical collaboration of mllm agents. *arXiv preprint arXiv:2503.10200* (2025).

[7] Zhenfang Chen, Rui Sun, Wenjun Liu, Yining Hong, and Chuang Gan. 2023. Genome: generative neuro-symbolic visual reasoning by growing and reusing modules. *arXiv preprint arXiv:2311.04901* (2023).

[8] Zhe Chen, Jiannan Wu, Wenhui Wang, Weijie Su, Guo Chen, Sen Xing, Muyan Zhong, Qinglong Zhang, Xizhou Zhu, Lewei Lu, et al. 2024. Internvl: Scaling up vision foundation models and aligning for generic visual-linguistic tasks. In *Proceedings of the IEEE/CVF Conference on Computer Vision and Pattern Recognition*. 24185–24198.

[9] Chaoyou Fu, Peixian Chen, Yunhang Shen, Yulei Qin, Mengdan Zhang, Xu Lin, Jinrui Yang, Xiawu Zheng, Ke Li, Xing Sun, Yunsheng Wu, and Rongrong Ji. 2024. MME: A Comprehensive Evaluation Benchmark for Multimodal Large Language Models. *arXiv:2306.13394* [cs.CV] <https://arxiv.org/abs/2306.13394>

[10] Team GLM, Aohan Zeng, Bin Xu, Bowen Wang, Chenhui Zhang, Da Yin, Dan Zhang, Diego Rojas, Guanyu Feng, Hanlin Zhao, et al. 2024. Chatglm: A family of large language models from glm-130b to glm-4 all tools. *arXiv preprint arXiv:2406.12793* (2024).

[11] Yash Goyal, Tejas Khot, Douglas Summers-Stay, Dhruv Batra, and Devi Parikh. 2017. Making the v in vqa matter: Elevating the role of image understanding in visual question answering. In *Proceedings of the IEEE conference on computer vision and pattern recognition*. 6904–6913.

[12] Aaron Grattafiori, Abhimanyu Dubey, and et.al. Abhinav Jauhri. 2024. The Llama 3 Herd of Models. *arXiv:2407.21783* [cs.AI] <https://arxiv.org/abs/2407.21783>

[13] Tammay Gupta and Aniruddha Kembhavi. 2023. Visual programming: Compositional visual reasoning without training. In *Proceedings of the IEEE/CVF Conference on Computer Vision and Pattern Recognition*. 14953–14962.

[14] Ronghang Hu, Jacob Andreas, Trevor Darrell, and Kate Saenko. 2018. Explainable neural computation via stack neural module networks. In *Proceedings of the European conference on computer vision (ECCV)*. 53–69.

[15] Ronghang Hu, Jacob Andreas, Marcus Rohrbach, Trevor Darrell, and Kate Saenko. 2017. Learning to Reason: End-To-End Module Networks for Visual Question Answering. In *Proceedings of the IEEE International Conference on Computer Vision (ICCV)*.

[16] Drew A Hudson and Christopher D Manning. 2019. Gqa: A new dataset for real-world visual reasoning and compositional question answering. In *Proceedings of the IEEE/CVF conference on computer vision and pattern recognition*. 6700–6709.

[17] Minyoung Huh, Brian Cheung, Tongzhou Wang, and Phillip Isola. 2024. The Platonic Representation Hypothesis. In *ICML*.

[18] Albert Q. Jiang, Alexandre Sablayrolles, Arthur Mensch, Chris Bamford, Devendra Singh Chaplot, Diego de las Casas, Florian Bressand, Gianna Lengyel, Guillaume Lampe, Lucile Saulnier, Lélio Renard Lavaud, Marie-Anne Lachaux, Pierre Stock, Teven Le Scao, Thibaut Lavril, Thomas Wang, Timothée Lacroix, and William El Sayed. 2023. Mistral 7B. *arXiv:2310.06825* [cs.CL] <https://arxiv.org/abs/2310.06825>

[19] Justin Johnson, Bharath Hariharan, Laurens Van Der Maaten, Judy Hoffman, Li Fei-Fei, C Lawrence Zitnick, and Ross Girshick. 2017. Inferring and executing programs for visual reasoning. In *Proceedings of the IEEE international conference on computer vision*. 2989–2998.

[20] Sahar Kazemzadeh, Vicente Ordonez, Mark Matten, and Tamara Berg. 2014. ReferItGame: Referring to Objects in Photographs of Natural Scenes. In *Proceedings of the 2014 Conference on Empirical Methods in Natural Language Processing (EMNLP)*, Alessandro Moschitti, Bo Pang, and Walter Daelemans (Eds.). Association for Computational Linguistics, Doha, Qatar, 787–798. <https://doi.org/10.3115/v1/D14-1086>

[21] Wonjae Kim, Bokyung Son, and Ildoo Kim. 2021. Vilt: Vision-and-language transformer without convolution or region supervision. In *International conference on machine learning*. PMLR, 5583–5594.

[22] Xin Lai, Zhuotao Tian, Yukang Chen, Yanwei Li, Yuhui Yuan, Shu Liu, and Jiaya Jia. 2024. Lisa: Reasoning segmentation via large language model. In *Proceedings of the IEEE/CVF Conference on Computer Vision and Pattern Recognition*. 9579–9589.

[23] Junnan Li, Dongxu Li, Caiming Xiong, and Steven Hoi. 2022. Blip: Bootstrapping language-image pre-training for unified vision-language understanding and generation. In *International conference on machine learning*. PMLR, 12888–12900.

[24] Zhaowei Li, Qi Xu, Dong Zhang, Hang Song, YiQing Cai, Qi Qi, Ran Zhou, Junting Pan, Zefeng Li, Vu Tu, Zhida Huang, and Tao Wang. 2024. GroundingGPT: Language Enhanced Multi-modal Grounding Model. In *Proceedings of the 62nd Annual Meeting of the Association for Computational Linguistics (Volume 1: Long Papers)*, Lun-Wei Ku, Andre Martins, and Vivek Srikumar (Eds.). Association for Computational Linguistics, Bangkok, Thailand, 6657–6678. <https://doi.org/10.18653/v1/2024.acl-long.360>

[25] Ziyi Lin, Chris Liu, Renrui Zhang, Peng Gao, Longtian Qiu, Han Xiao, Han Qiu, Chen Lin, Wenqi Shao, Keqin Chen, et al. 2023. Sphinx: The joint mixing of weights, tasks, and visual embeddings for multi-modal large language models. *arXiv preprint arXiv:2311.07575* (2023).

[26] Shilong Liu, Zhaoyang Zeng, Tianhe Ren, Feng Li, Hao Zhang, Jie Yang, Chunyu Li, Jianwei Yang, Hang Su, Jun Zhu, and Lei Zhang. 2023. Grounding DINO: Marrying DINO with Grounded Pre-Training for Open-Set Object Detection. *arXiv:2303.05499* [cs.CV]

[27] J MacQueen. 1967. Multivariate observations. In *Proceedings of the 5th Berkeley Symposium on Mathematical Statistics and Probability*, Vol. 1. 281–297.

[28] Juhong Min, Shyamal Buch, Arsha Nagrani, Minsu Cho, and Cordelia Schmid. 2024. MoRevQA: Exploring Modular Reasoning Models for Video Question Answering. In *Proceedings of the IEEE Conference on Computer Vision and Pattern Recognition (CVPR)*.

[29] Matthias Minderer, Alexey Gritsenko, and Neil Houlsby. 2023. Scaling open-vocabulary object detection. *Advances in Neural Information Processing Systems* 36 (2023), 72983–73007.

[30] OpenAI. 2023. GPT-4 Technical Report. Technical Report. OpenAI.

[31] Zhihang Peng, Wenhui Wang, Li Dong, Yaru Hao, Shaohan Huang, Shuming Ma, Qixiang Ye, and Furui Wei. 2024. Grounding Multimodal Large Language Models to the World. In *The Twelfth International Conference on Learning Representations*. <https://openreview.net/forum?id=ILmqxkfSIw>

[32] Hanooza Rasheed, Muhammad Maaz, Sahal Shahji, Abdelrahman Shaker, Salman Khan, Hisham Cholakkal, Rao M Anwer, Eric Xing, Ming-Hsuan Yang, and Fahad S Khan. 2024. Glamm: Pixel grounding large multimodal model. In *Proceedings of the IEEE/CVF Conference on Computer Vision and Pattern Recognition*. 13009–13018.

[33] Zhongwei Ren, Zhicheng Huang, Yunchao Wei, Yao Zhao, Dongmei Fu, Jiashi Feng, and Xiaojie Jin. 2024. Pixelmm: Pixel reasoning with large multimodal model. In *Proceedings of the IEEE/CVF Conference on Computer Vision and Pattern Recognition*. 26374–26383.

[34] Peter J Rousseeuw. 1987. Silhouettes: a graphical aid to the interpretation and validation of cluster analysis. *Journal of computational and applied mathematics* 20 (1987), 53–65.

[35] Chuyi Shang, Amos You, Sanjay Subramanian, Trevor Darrell, and Roei Herzig. 2024. TraveLER: A Modular Multi-LMM Agent Framework for Video Question-Answering. *arXiv:2404.01476* [cs.CV] <https://arxiv.org/abs/2404.01476>

[36] Pratyusha Sharma, Tamar Rott Shaham, Manel Baradad, Stephanie Fu, Adrian Rodriguez-Munoz, Shivam Duggal, Phillip Isola, and Antonio Torralba. 2024. TA Vision Check-up for Language Models. In *CVPR*.

[37] Ishika Singh, Valts Blukis, Arsalan Mousavian, Ankit Goyal, Danfei Xu, Jonathan Tremblay, Dieter Fox, Jesse Thomason, and Animesh Garg. 2023. ProgPrompt: Generating Situated Robot Task Plans using Large Language Models. In *2023 IEEE International Conference on Robotics and Automation (ICRA)*. 11523–11530. <https://doi.org/10.1109/ICRA48891.2023.10161317>

[38] Andreas Steiner, André Susano Pinto, Michael Tschannen, Daniel Keysers, Xiao Wang, Yonatan Bitton, Alexey Gritsenko, Matthias Minderer, Anthony Sherbondy, Shanghang Long, et al. 2024. Paligemma 2: A family of versatile vlms for transfer. *arXiv preprint arXiv:2412.03555* (2024).

[39] Alane Suhr, Stephanie Zhou, Ally Zhang, Iris Zhang, Huajun Bai, and Yoav Artzi. 2018. A corpus for reasoning about natural language grounded in photographs. *arXiv preprint arXiv:1811.00491* (2018).

[40] Didae Suris, Sachit Menon, and Carl Vondrick. 2023. Vipergrpt: Visual inference via python execution for reasoning. In *Proceedings of the IEEE/CVF International Conference on Computer Vision*. 11888–11898.

[41] Peng Wang, An Yang, Rui Men, Junyang Lin, Shuai Bai, Zhikang Li, Jianxin Ma, Chang Zhou, Jingren Zhou, and Hongxia Yang. 2022. OFA: Unifying Architectures, Tasks, and Modalities Through a Simple Sequence-to-Sequence Learning Framework. *CoRR* abs/2202.03052 (2022).

[42] Weiyun Wang, Zhangwei Gao, Lixin Gu, Hengjun Pu, Long Cui, Xingguang Wei, Zhaoyang Liu, Linglin Jing, Shenglong Ye, Jie Shao, et al. 2025. InternVL3.5.

Advancing Open-Source Multimodal Models in Versatility, Reasoning, and Efficiency. *arXiv preprint arXiv:2508.18265* (2025).

[43] Xiaohan Wang, Yuhui Zhang, Orr Zohar, and Serena Yeung-Levy. 2024. VideoAgent: Long-form Video Understanding with Large Language Model as Agent. *European Conference on Computer Vision (ECCV)* (2024).

[44] Fangyun Wei, Jinjing Zhao, Kun Yan, Hongyang Zhang, and Chang Xu. 2025. A large-scale human-centric benchmark for referring expression comprehension in the LMM era. In *Proceedings of the 38th International Conference on Neural Information Processing Systems* (Vancouver, BC, Canada) (NIPS '24). Curran Associates Inc., Red Hook, NY, USA, Article 2222, 22 pages.

[45] Bin Xiao, Haiping Wu, Weijian Xu, Xiyang Dai, Houdong Hu, Yumao Lu, Michael Zeng, Ce Liu, and Lu Yuan. 2024. Florence-2: Advancing a Unified Representation for a Variety of Vision Tasks. In *Proceedings of the IEEE/CVF Conference on Computer Vision and Pattern Recognition (CVPR)*. 4818–4829.

[46] Junbin Xiao, Xindi Shang, Angela Yao, and Tat-Seng Chua. 2021. NExT-QA: Next Phase of Question-Answering to Explaining Temporal Actions. In *Proceedings of the IEEE/CVF Conference on Computer Vision and Pattern Recognition (CVPR)*. 9777–9786.

[47] Zhengyuan Yang, Zhe Gan, Jianfeng Wang, Xiaowei Hu, Yumao Lu, Zicheng Liu, and Lijuan Wang. 2022. An Empirical Study of GPT-3 for Few Short Knowledge-based VQA. *AAAI* (2022).

[48] Yuan Yao, Tianyu Yu, Ao Zhang, Chongyi Wang, Junbo Cui, Hongji Zhu, Tianchi Cai, Haoyu Li, Weilin Zhao, Zhihui He, et al. 2025. MiniCPM-V: A GPT-4V Level MLLM on Your Phone. *Nat Commun* 16, 5509 (2025) (2025).

[49] Haoxuan You, Haotian Zhang, Zhe Gan, Xianzhi Du, Bowen Zhang, Zirui Wang, Liangliang Cao, Shih-Fu Chang, and Yinfei Yang. 2023. Ferret: Refer and Ground Anything Anywhere at Any Granularity. *arXiv preprint arXiv:2310.07704* (2023).

[50] Shoubin Yu, Jaemin Cho, Prateek Yadav, and Mohit Bansal. 2023. Self-Chained Image-Language Model for Video Localization and Question Answering. In *NeurIPS*.

[51] Boqiang Zhang, Kehan Li, Zesen Cheng, Zhiqiang Hu, Yuqian Yuan, Guanzheng Chen, Sicong Leng, Yuming Jiang, Hang Zhang, Xin Li, Peng Jin, Wenqi Zhang, Fan Wang, Lidong Bing, and Deli Zhao. 2025. VideoLLaMA 3: Frontier Multi-modal Foundation Models for Image and Video Understanding. *arXiv preprint arXiv:2501.13106* (2025). <https://arxiv.org/abs/2501.13106>

[52] Yuanhan Zhang, Bo Li, haotian Liu, Yong jae Lee, Liangke Gui, Di Fu, Jiashi Feng, Ziwei Liu, and Chunyuan Li. 2024. LLaVA-NeXT: A Strong Zero-shot Video Understanding Model. <https://llava-vl.github.io/blog/2024-04-30-llava-next-video/>

[53] Yuanhan Zhang, Jinming Wu, Wei Li, Bo Li, Zejun Ma, Ziwei Liu, and Chunyuan Li. 2024. Video Instruction Tuning With Synthetic Data. *arXiv:2410.02713 [cs.CV]* <https://arxiv.org/abs/2410.02713>

[54] Zheng Zhang, Yeyao Ma, Enming Zhang, and Xiang Bai. 2024. Psalm: Pixelwise segmentation with large multi-modal model. In *European Conference on Computer Vision*. Springer, 74–91.